



CETP Inhibition Improves HDL Function but Leads to Fatty Liver and Insulin Resistance in CETP-Expressing Transgenic Mice on a High-Fat Diet

Lin Zhu,^{1,2} Thao Luu,² Christopher H. Emfinger,^{1,2} Bryan A. Parks,³ Jeanne Shi,^{2,4} Elijah Trefts,⁵ Fenghua Zeng,⁶ Zsuzsanna Kuklennyik,³ Raymond C. Harris,⁶ David H. Wasserman,⁵ Sergio Fazio,⁷ and John M. Stafford^{1,2,5}

Diabetes 2018;67:2494–2506 | <https://doi.org/10.2337/db18-0474>

In clinical trials, inhibition of cholesteryl ester transfer protein (CETP) raises HDL cholesterol levels but does not robustly improve cardiovascular outcomes. Approximately two-thirds of trial participants are obese. Lower plasma CETP activity is associated with increased cardiovascular risk in human studies, and protective aspects of CETP have been observed in mice fed a high-fat diet (HFD) with regard to metabolic outcomes. To define whether CETP inhibition has different effects depending on the presence of obesity, we performed short-term anacetrapib treatment in chow- and HFD-fed CETP transgenic mice. Anacetrapib raised HDL cholesterol and improved aspects of HDL functionality, including reverse cholesterol transport, and HDL's antioxidative capacity in HFD-fed mice was better than in chow-fed mice. Anacetrapib worsened the anti-inflammatory capacity of HDL in HFD-fed mice. The HDL proteome was markedly different with anacetrapib treatment in HFD- versus chow-fed mice. Despite benefits on HDL, anacetrapib led to liver triglyceride accumulation and insulin resistance in HFD-fed mice. Overall, our results support a physiologic importance of CETP in protecting from fatty liver and demonstrate context selectivity of CETP inhibition that might be important in obese subjects.

HDL particles have important antiatherosclerotic functions (1). HDL particles accept cholesterol from peripheral

tissues, including the arterial walls, for delivery to the liver in a process termed reverse cholesterol transport (1). Antioxidative effects of HDL prevent LDL oxidation (oxLDL), which are more efficient in initiating atheroma formation when trapped in the subendothelial space (1,2). HDL particles also protect endothelial cells from inflammation induced by exposure to oxLDL (3–5). The Framingham Heart Study and other prospective population studies have established that HDL cholesterol is inversely correlated with cardiovascular disease (CVD) risk, and low HDL cholesterol levels are recognized as an independent risk factor for CVD. Thus, efforts to increase HDL cholesterol and improve HDL functionality have been a focus of pharmaceutical development with the aim of reducing CVD risk.

In humans, cholesteryl ester transfer protein (CETP) shuttles cholesteryl esters and triglycerides (TGs) between serum lipoproteins, including HDL, LDL, and VLDL. CETP-mediated shuttling of TGs into HDL accelerates clearance of HDL's scaffold protein apolipoprotein (apo) A1, which may further lower levels of HDL cholesterol in addition to shifting cholesteryl ester from HDL to apoB-containing lipoproteins (6). CETP inhibition has been pursued as an approach to increase HDL cholesterol and reduce CVD risk. Clinical trials largely have not shown that CETP inhibition reduces CVD risk (7–9), although recently, anacetrapib

¹Veterans Administration Tennessee Valley Healthcare System, Vanderbilt University School of Medicine, Nashville, TN

²Division of Diabetes, Endocrinology, and Metabolism, Vanderbilt University School of Medicine, Nashville, TN

³Division of Laboratory Sciences, Centers for Disease Control and Prevention, Atlanta, GA

⁴Trinity College of Art and Science, Duke University, Durham, NC

⁵Department of Molecular Physiology and Biophysics, Vanderbilt University School of Medicine, Nashville, TN

⁶Division of Nephrology and Hypertension, Vanderbilt University School of Medicine, Nashville, TN

⁷The Center for Preventive Cardiology at the Knight Cardiovascular Institute, Oregon Health & Science University, Portland, OR

Corresponding author: John M. Stafford, john.stafford@vanderbilt.edu.

Received 26 April 2018 and accepted 5 September 2018.

This article contains Supplementary Data online at <http://diabetes.diabetesjournals.org/lookup/suppl/doi:10.2337/db18-0474/-/DC1>.

© 2018 by the American Diabetes Association. Readers may use this article as long as the work is properly cited, the use is educational and not for profit, and the work is not altered. More information is available at <http://www.diabetesjournals.org/content/license>.

showed modest CVD risk reduction after a long follow-up (10). Of note, approximately two-thirds of patients in clinical trials with CETP inhibitors were obese. Obesity and hyperlipidemia are known to significantly affect aspects of cholesterol metabolism and HDL biology (11) and might affect aspects of CETP-mediated biology. Human studies have shown that higher plasma CETP is associated with a reduced risk of CVD, depending on plasma TG levels or sex (12–14). Mice naturally lack CETP and have high levels of HDL cholesterol, one of the likely reasons why they are relatively resistant to atherosclerosis. Similar to observations in human studies, transgenic expression of CETP in mice increased atherosclerotic burden in some studies (15,16), yet limited atherosclerosis progression in others (17,18). We have shown that transgenic expression of CETP in mice reduces liver fat content and improves insulin sensitivity in diet-induced obese mice (19,20). These studies suggested that CETP's action relates to CVD, and effects of CETP inhibition may be metabolically context dependent.

We propose that the effects of CETP inhibition on HDL protein composition and functionality are influenced by obesity and hyperlipidemia that result from high-fat diet (HFD) feeding. We report that treatment with the CETP inhibitor anacetrapib increased HDL cholesterol independent of diet. However, HFD feeding had a large impact on the effects of CETP inhibition on the HDL proteome and HDL functionality. In addition, in diet-induced obese mice, CETP inhibition modified control of several steps in liver lipid metabolism, increased liver TG content, increased liver inflammation, and worsened liver insulin resistance.

RESEARCH DESIGN AND METHODS

CETP Inhibition by Anacetrapib in CETP Transgenic Mice

CETP transgenic mice on a C57BL/6 genetic background [C57BL/6-Tg(CETP)UCTP20Pnu/J, International Mouse Strain Resource Cat# JAX:001929] were purchased from The Jackson Laboratory. For the first cohort, one group of male CETP transgenic mice were kept on chow diet, whereas the second group was placed on an HFD (60% fat, 20% protein) (D08060104; Research Diets) for 3 months. Mice then were administered with anacetrapib or vehicle according to Tan et al. (21). Anacetrapib was from MedChemExpress (Cat# HY-12090). Anacetrapib is hydrophobic, so to avoid potential differences in oral absorption depending on whether mice were chow or HFD fed, we administered the dose intravenously. The intravenous dose of anacetrapib was formulated in polyethylene glycol 400/water (6/4 vol/vol) at a concentration of 0.2 mg/mL. Each mouse received a dose of 2.5 mL/kg by intravenous injection through the suborbital vein. Our preliminary data showed that the $t_{1/2}$ was 11.8 h, so anacetrapib was injected intravenously every 12 h for five doses. After the last injection in the morning, mice were fasted for 5 h and sacrificed, and serum and tissues were collected and stored at -80°C . All procedures were

performed in accordance with the National Institutes of Health (NIH) *Guidelines for the Care and Use of Laboratory Animals* and were approved by the institutional animal care and use committee at Vanderbilt University.

High-Performance Liquid Chromatography and Serum Lipid Assays

We used size exclusion chromatography (SEC) with a high-performance liquid chromatography (HPLC) system to separate plasma lipids to quantify the distribution of lipoproteins and define the composition of HDL. The SEC separation was performed as previously described (22). Cholesterol content was assayed from fractions using Raichem reagent (Cat# R80035; Cliniaq). VLDL was defined as fractions 8–14, LDL as fractions 15–29, and HDL as fractions 30–40. Plasma (5 μL) was diluted 1:10 and assayed for total cholesterol levels and was diluted 1:25 for TG assay using commercially available kits (Cliniaq).

HDL Proteomic Analysis

SEC/HPLC fractions for HDL (fractions 30–40) (Fig. 2A and B) were used for HDL proteomics analysis. Apos A1, A2, A4, C1, E, and M; lecithin cholesterol acyltransferase (LCAT); lipoprotein lipase (LPL); phospholipid transfer protein (PLTP); paraoxonase I (PON1); and serum amyloid A1 (SAA1) in each 100- μL SEC fraction were analyzed by multiple reaction monitoring (MRM) and mass spectrometry (MS). The MRM-MS workstation included an integrated online trypsin digestion-coupled liquid chromatography (LC) system (Perfinity Biosciences, West Lafayette, IN) and a mass spectrometer (QTRAP 6500; SCIEX, Framingham, MA). To each fraction, 50 μL of 0.45% Zwittergent 3-12 detergent was added to a nominal concentration of 0.15% in the well. The sample plate was mixed on a plate shaker for 2 min at 500 rpm and placed directly into the autosampler held at 8°C . Fifty microliters of sample was injected onto the workstation. Full details can be found in a previous publication (23).

The online digestion took place on a trypsin column (2.1 \times 33 mm) operating at 50°C with a 25 $\mu\text{L}/\text{min}$ flow rate. The cleavage products were carried together directly to the trapping column (Halo C18 4.6 \times 5 mm, 2.7- μm guard column). After the digestion/trapping period, the cleavage products were eluted from the trapping column to the analytical column (Halo C18 2.1 \times 100 mm, 2.7- μm core shell HPLC column). The analytical separation was performed at 50°C with a flow rate of 350 $\mu\text{L}/\text{min}$ over a stepwise gradient ranging from 3 to 95% acetonitrile containing 0.1% formic acid. The total analysis time for each injection was 12 min. The target peptide masses were acquired with unit mass resolution in retention time scheduled MRM mode with 60-s acquisition windows and 0.65-s target scan time. Protein-specific peptides were derived from UniProt sequences (*Mus musculus*) (www.uniprot.org). Skyline 3.1 software (<https://skyline.ms/project/home/software/Skyline/begin.view>) was used for generation of the LC tandem MS acquisition method files. The relative concentration of each protein was

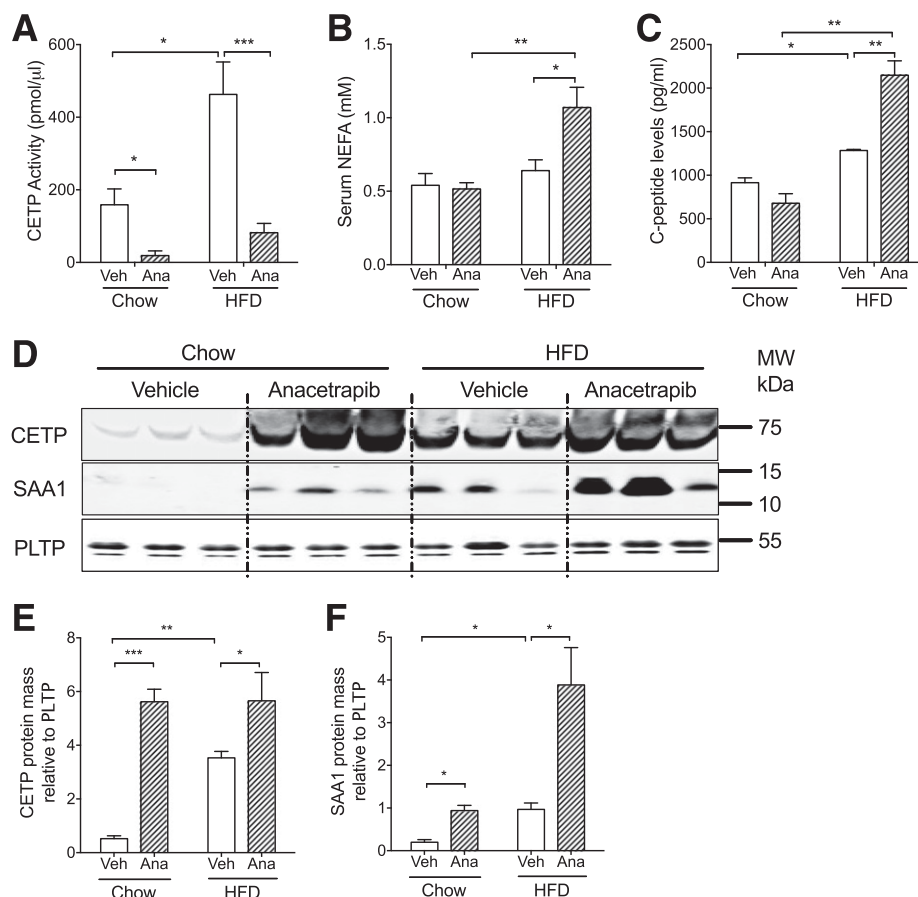


Figure 1—Anacetrapib inhibited CETP activity and was associated with increased insulin secretion and inflammation in HFD-fed mice. **A:** CETP enzymatic activity was increased by HFD and was suppressed by anacetrapib in chow- and HFD-fed mice. **B:** Serum NEFA levels were increased by anacetrapib treatment in HFD-fed CETP mice. **C:** C-peptide levels were increased by diet and anacetrapib treatment. **D:** Western blots for CETP and SAA1 proteins in serum. Membranes for SAA1 were stripped and reprobed with the PLTP antibody. Molecular weight (MW) positions (Bio-Rad Precision Plus Protein Kaleidoscope Standards) are shown. **E:** Quantification of Western blots for serum CETP ($n \geq 6$). **F:** Quantification of Western blots for serum SAA1 ($n \geq 6$). Significant differences were determined using repeated-measures by both factors two-way ANOVA with Bonferroni multiple comparison test. * $P < 0.05$, ** $P < 0.01$, *** $P < 0.001$. Ana, anacetrapib; Veh, vehicle.

determined from LC-MS peak areas of at least two signature peptides (Supplementary Table 1) and was normalized by HDL protein.

Serum Enzyme Activity Assays

Serum enzyme activities were determined using a commercially available kit. CETP enzyme activity was assayed using a cell-free assay according to the manufacturer's protocol (Roar Biomedical).

LCAT activity assays were performed with an LCAT Activity Assay Kit (Fluorometric) from Cell Biolabs (Cat# STA-615). Whole-serum lipase activity was evaluated using Lipase Activity Assay Kit III from Sigma-Aldrich (Cat# MAK048), and PLTP activity assays were performed using PLTP Activity Assay Kit from Sigma-Aldrich (Cat# MAK108).

In Vitro Cellular Cholesterol Efflux Assays

The in vitro reverse cholesterol transport assays were performed as described previously (22,24). Preparation of HDL particles from each group and generation of

radiolabeled foam cells derived from wild-type (WT) female mice were performed as we previously described (22). Peritoneal macrophages from WT mice were collected 72 h after intraperitoneal injection of thioglycollate. Macrophages were first cultured in DMEM with 10% FBS for 2 h to allow for plate surface attachment and then cultured in DMEM with 0.2% BSA overnight. The next day, macrophages were loaded with 2 $\mu\text{Ci}/\text{mL}$ ^3H -cholesterol and 25 $\mu\text{g}/\text{mL}$ acetylated LDL for 48 h. These labeled foam cells were washed twice and equilibrated in medium with 0.2% BSA for 2 h, and a set of cells were collected for ^3H -radioactivity in cells. According to the dose-response curves (Supplementary Fig. 4A), the rest of the cells were treated with 1% of the initial serum in DMEM with 0.2% BSA. Cells treated only with DMEM with 0.2% BSA were used as a negative control, and cells treated with apoA1 (30 $\mu\text{g}/\text{mL}$ [Meridian Life Science]) (Supplementary Fig. 4A) were used as the positive control. Media (120 μL) were collected at times 1, 2, and 4 h. The media were filtered, and 100 μL was used for the determination

of ^3H -radioactivities in media using liquid scintillation counting for cholesterol efflux calculation.

Antioxidative Function of HDL for oxLDL

Kinetics of oxLDL in the presence of HDL was performed according to Qin et al. (2). One microgram HDL purified from each experimental mouse was added in 300 μL reaction mix containing 30 μg LDL (Alfa Aesar) and 20 $\mu\text{mol/L}$ CuSO_4 in Dulbecco's PBS. Human HDL particles from Cell Biolabs (Cat# STA-243) were used for dose-response curve analysis and as positive control, and reaction without HDL was used as blank (Supplementary Fig. 4C). Reaction solutions were incubated at 37°C for up to 3 h in a plate reader. Absorbance readings at 234 nm were taken every minute to measure formation of conjugated dienes.

Anti-inflammatory Function of HDL in oxLDL-Treated Endothelial Cells

Human coronary artery endothelial cells (CC-2585; Lonza, Walkersville, MD) were grown in EGM-2MV BulletKit Medium (Lonza) containing 10% vol/vol FBS and plated 24 h before use in 12-well plates at a density of 1×10^5 cells/well. Cells were incubated at 37°C for 4 h with oxLDL (80 $\mu\text{g/mL}$ [Alfa Aesar]) and then washed twice with PBS and treated with HDL (5% vol/vol) in media containing 10% of lipoprotein-deficient bovine serum (Alfa Aesar) for 36 h (results of titration experiments shown in Supplementary Fig. 5A). Cells were then washed and RNAs isolated using RNeasy Mini Kit (QIAGEN). cDNA was synthesized using the qScript cDNA synthesis kit (Quantabio). Real-time PCR was performed using TaqMan Fast Universal PCR Master Mix (2X) and TaqMan gene expression assays (Life Technologies) (Supplementary Table 2) on the QuantStudio 12K Flex Real-Time PCR System (Applied Biosystems).

Liver Lipids and mRNA Quantification

Liver lipid profiles were analyzed at the Vanderbilt University Medical Center Lipid Core. Total RNA was isolated from ~50 mg of snap-frozen tissues using RNeasy Mini Kit. cDNA was synthesized, and real-time PCR was performed as described above. Assays for determination of mRNA levels of inflammatory markers are listed in Supplementary Table 2.

VLDL-TG Secretion

CETP male mice were fed an HFD for 1 month and treated with anacetrapib and vehicle by intravenous injection through the suborbital vein every 12 h for five doses. Mice were fasted for 3 h and were given 500 mg/kg tyloxapol intravenously. Plasma TGs were measured from tail blood sampling over 3 h after tyloxapol administration.

Western Blots

Western blotting for liver proteins was performed as reported previously (25). Primary antibody for apoB was from L. Swift of Vanderbilt University School of Medicine (26). Primary antibody for CETP was from Abcam (ab-51771), rabbit anti-mouse apoA1 was from Meridian Life Science (K23500R), antibody for apoM was from Cell

Signaling (5709S), goat anti-mSAA1 was from R&D Systems (AF2948), antibody for LDL receptor was from Abcam (ab30532), rabbit polyclonal anti-PLTP antibody was from Abcam (ab189776), and rabbit anti-actin (I-19) antibody was from Santa Cruz (sc-1616). Secondary antibodies were from LI-COR (Lincoln, NE). All primary antibodies were diluted 1:1,000, except where noted. All secondary antibodies were diluted 1:10,000. Images were acquired using a LI-COR Odyssey infrared imaging.

Fatty Acid Oxidation in Primary Hepatocytes

After chow or HFD feeding for 1 month, CETP transgenic male mice were treated with anacetrapib or vehicle by intravenous injection through the suborbital vein every 12 h for five doses ($n = 4$). Within 3 h of the last injection of the drug or vehicle, primary hepatocytes were isolated and cultured as described before (22). Briefly, mice were anesthetized, and livers were perfused with the perfusion buffer (KCl 7 mmol/L, NaHPO_4 0.7 mmol/L, NaCl 137 mmol/L, HEPES 10 mmol/L, EGTA 500 mmol/L, CaCl_2 2.38 mmol/L, pH 7.4) through the inferior vena cava while the superior vena cava was clamped and portal vein was cut. After the liver was washed, perfusion buffer was switched to digestion buffer containing collagenase (Cat# 5138; Sigma) for ~5–8 min. The liver was removed, and hepatocytes were washed and seed in 24-well plates (10^6 cells/well) in M199 media containing glutamax, penicillin-streptomycin, 10% FCS, 10 nmol/L insulin, 200 nmol/L triiodothyronine, and 500 nmol/L dexamethasone. When attached to the bottom after 4–6 h of culturing, cells were subjected to fatty acid oxidation assay.

Ex vivo fatty acid oxidation assay was performed according to Hirschey and Verdin (27). Fatty acid oxidation was studied using [$1\text{-}^{14}\text{C}$]palmitate (Cat# NEC075H; PerkinElmer) in the presence of unlabeled palmitate (100 $\mu\text{mol/L}$). Both [$1\text{-}^{14}\text{C}$]palmitate and unlabeled palmitate were first bound to 2% wt/vol fatty-acid-free BSA and then added to media at the final concentration of 0.3% BSA, 100 $\mu\text{mol/L}$ unlabeled palmitate, and 2 μCi [$1\text{-}^{14}\text{C}$]palmitate per reaction. The fatty acid oxidation was performed in culturing media without insulin in a 37°C CO_2 incubator for 30 min according to the time course responses (Supplementary Fig. 5B). The assay was stopped by adding 400 μL 5% perchloric acid. The ^{14}C -labeled acid-soluble products were determined using scintillation counting. Rotenone at the final concentration of 100 nmol/L was used as the fatty acid oxidation inhibitor for negative control.

Euglycemic-Hyperinsulinemic Clamp Study

The second cohort of mice comprised 12-week-old CETP females fed an HFD for 3 months. The carotid artery and jugular vein were catheterized at the Mouse Metabolic Phenotyping Center at Vanderbilt University Medical Center as described previously (25). Anacetrapib was given to the mice through the jugular vein catheter for 5 days, and mice treated with vehicle were used as control. Euglycemia (~150 mg/dL) was maintained by measuring blood glucose every 10 min starting at $t = 0$ min and adjusting the infusion

of 50% dextrose as necessary. Mice received saline-washed erythrocytes from donors to prevent a fall in hematocrit. Blood was collected every 5 min until $t = 145$ min when mice were sacrificed and tissues flash frozen.

Systolic Blood Pressure

The third cohort of mice comprised CETP transgenic males fed an HFD for 5 months. These mice then were administered anacetrapib or vehicle by intravenous injection through the suborbital vein every 12 h for 3 weeks. During the last week of drug treatment, systolic blood pressure (SBP) was measured in conscious mice at room temperature using a tail-cuff monitor (BP-2000 Blood Pressure Analysis System; Visitech Systems). Twelve-week-old male CETP transgenic mice fed a chow diet were used as controls for SBP. SBP for each mouse was the mean value of the last 4 days of measurements.

Statistical Analysis

All measurements passed a D'Agostino and Pearson omnibus normality test ($\alpha = 0.05$). Data are presented as mean \pm SD unless otherwise indicated. Differences between groups were determined by ANOVA followed by multiple comparison tests or by Student t test with Welch correction as appropriate. Significance was flagged by $P < 0.05$.

RESULTS

CETP Inhibition Modifies HDL Functionality and Increases Insulin Secretion Only in Diet-Induced Obese Mice

CETP transgenic mice fed a chow diet or HFD were treated with anacetrapib every 12 h for five doses, and mice treated with the vehicle were used as controls. HFD feeding increased body weight and adiposity as well as blood glucose, cholesterol, TGs, insulin, leptin, interleukin (IL)-6, and resistin in fasting animals (Table 1). CETP activity was increased by 192% by HFD feeding,

concomitant with the increase in CETP protein levels with HFD feeding (Fig. 1A, D, and E). Anacetrapib inhibited CETP activity by 89% in chow-fed mice and by 83% in HFD-fed mice (Fig. 1A). Serum CETP mass was increased in anacetrapib-treated mice (Fig. 1D and E), which was consistent with a previous report that anacetrapib treatment increases CETP mass in circulation (28). SAA1, an inflammatory factor, was increased by HFD feeding and CETP inhibition (Fig. 1D and F). Blood levels of nonesterified fatty acid (NEFA), IL-6, and resistin were concomitantly increased by anacetrapib in HFD-fed obese mice (Fig. 1B and Table 1). Serum C-peptide levels were increased by 40% by HFD feeding and further increased by 67% by anacetrapib treatment only in HFD-fed mice, indicating insulin resistance in those mice (Fig. 1C). In a separate experiment, blood insulin levels were increased after an acute infusion of torcetrapib, another CETP inhibitor (Supplementary Fig. 1). Human studies showed that insulin secretion was stimulated with CETP inhibition, which is in line with our data (29,30).

HDL Particle Remodeling by Anacetrapib Is Different in Chow- and HFD-Fed Mice Concomitant With Changes in HDL Functionality

CETP inhibition by anacetrapib increased HDL cholesterol by 71% in chow-fed mice and by 172% in HFD-fed mice (Fig. 2A–C). HFD feeding increased TGs in LDL/IDL; anacetrapib did not change HDL-TGs in either chow- or HFD-fed mice (Fig. 2D–F).

Proteins comprise about one-half of the mass of HDL particles and contribute to HDL functionality with regard to cholesterol efflux and antioxidative and anti-inflammatory capacity. To better understand how HDL protein composition was modified by CETP inhibition in chow- and HFD-fed mice, we performed a proteomic analysis using HPLC fractions for HDL. In general, anacetrapib treatment resulted in greater changes to HDL's protein

Table 1—Physiologic characteristics related to lipid metabolism in chow- and HFD-fed mice

	Chow-fed		HFD-fed	
	Vehicle	Anacetrapib	Vehicle	Anacetrapib
Body weight (g)	25.5 \pm 1.3	26.1 \pm 1.7	36.2 \pm 4.7 [^]	42.5 \pm 5.5 [^]
Adiposity (%)	10.9 \pm 0.8	11.4 \pm 2.2	37.6 \pm 6.1 [^]	40.1 \pm 4.1 [^]
Blood				
Glucose (mg/dL)	63.4 \pm 17.1	63.7 \pm 7.8	91.2 \pm 11.8 [^]	87.7 \pm 14.7 [^]
Cholesterol (mg/dL)	68.5 \pm 13.4	101.5 \pm 10.4 [*]	116 \pm 4.2 [^]	118 \pm 3.8 [^]
TGs (mg/dL)	58.8 \pm 14.4	54.8 \pm 7.8	62.7 \pm 4.1 [^]	77.8 \pm 8.2 [^]
Insulin (pg/mL)	689 \pm 279	878 \pm 6	1,530 \pm 235 [^]	1,970 \pm 268 [^]
IL-6 (pg/mL)	137 \pm 31	189 \pm 29	196 \pm 65 [^]	323 \pm 77 ^{^*}
Resistin (pg/mL)	2,202 \pm 375	1,818 \pm 270	3,110 \pm 601 [^]	4,560 \pm 732 ^{^*}
Leptin (pg/mL)	530 \pm 287	304 \pm 107	3,582 \pm 547 [^]	5,183 \pm 2,154 [^]
LCAT activity (mU/mL)	305 \pm 39	348 \pm 33	336 \pm 67	389 \pm 26
LPL activity (mU/mL)	0.26 \pm 0.06	0.27 \pm 0.04	0.41 \pm 0.11 [^]	0.39 \pm 0.06 [^]
PLTP activity (pmol FIU transferred/mL)	160 \pm 14	150 \pm 5.9	183 \pm 1.2 [^]	199 \pm 12 [^]

Data are mean \pm SD. Statistical analysis was performed using two-way ANOVA with Bonferroni multiple comparison test. FIU, fluorescence intensity units. ^{*} $P < 0.05$ compared with respective vehicle controls. [^] $P < 0.05$ compared with chow-fed mice.

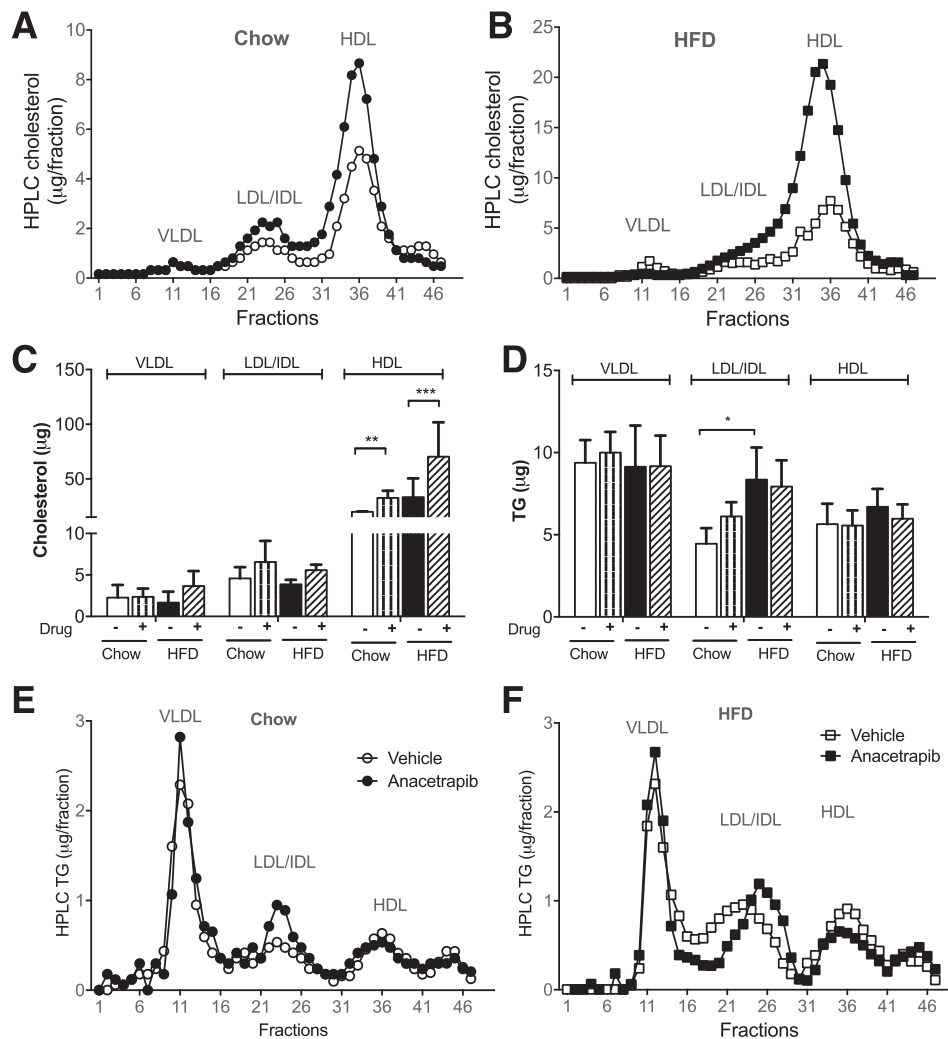


Figure 2—Anacetrapib modified lipid distribution of lipoproteins. *A* and *B*: Serum lipoproteins were separated by HPLC and cholesterol content of the fractions for chow- and HFD-fed mice. *C* and *D*: Bar graphs of lipoprotein cholesterol and TGs for each diet group. *E* and *F*: Lipoprotein TG content for chow- and HFD-fed mice. Significant differences were determined using repeated-measures by both factors two-way ANOVA with Bonferroni multiple comparison test ($n \geq 6$). * $P < 0.05$, ** $P < 0.01$, *** $P < 0.001$.

composition in HFD-fed obese CETP mice than in chow-fed CETP mice (Fig. 3). ApoA1, HDL's scaffold protein and the major cholesterol acceptor in HDL (31), was not changed by anacetrapib in chow-fed mice but increased by 657% ($P < 0.0001$) by anacetrapib compared with vehicle treatment in HFD-fed mice. Similar changes were seen for apoA2, which again was not changed by anacetrapib treatment in chow-fed mice but was increased by 640% ($P < 0.01$) by anacetrapib in HFD-fed mice compared with vehicle treatment (Fig. 3A). ApoA4, which may be involved in HDL's antioxidative capacity, also fell into the same pattern for HDL-apoA1 regulated by HFD feeding and anacetrapib. ApoE, a lipid transporter involved in multiple TG and cholesterol metabolic pathways, was increased by 284% ($P < 0.05$) by anacetrapib in chow-fed mice and was increased by 321% ($P < 0.05$) by anacetrapib in HFD-fed mice. ApoC1, a regulator for lipases and lipid transport that is activated during inflammation,

was slightly increased by anacetrapib in chow-fed mice and was increased by 7,414% (74-fold; $P < 0.05$) by anacetrapib in HFD-fed mice compared with vehicle-treated controls (Fig. 3A). ApoM, an antioxidant protein and an antiatherosclerotic factor that protects endothelial function, was not affected by anacetrapib in chow-fed mice but was increased by 879% ($P < 0.0001$) by anacetrapib in HFD-fed mice. PON1, another antioxidant protein in HDL, was not modified by anacetrapib in either group (Fig. 2A). SAA1, an inflammatory factor, was slightly increased by anacetrapib in chow-fed mice and was increased by 3,304% (33-fold; $P < 0.001$) by anacetrapib in HFD-fed mice (Fig. 2A). Unlike SAA1 levels in serum (Fig. 1D), SAA1 levels in HDL particles in HFD-fed vehicle-treated mice were not higher than in chow-fed vehicle-treated mice. These results suggest that SAA1 was also distributed in non-HDL particles when its level was raised by HFD. Proteomic analysis results were consistent with

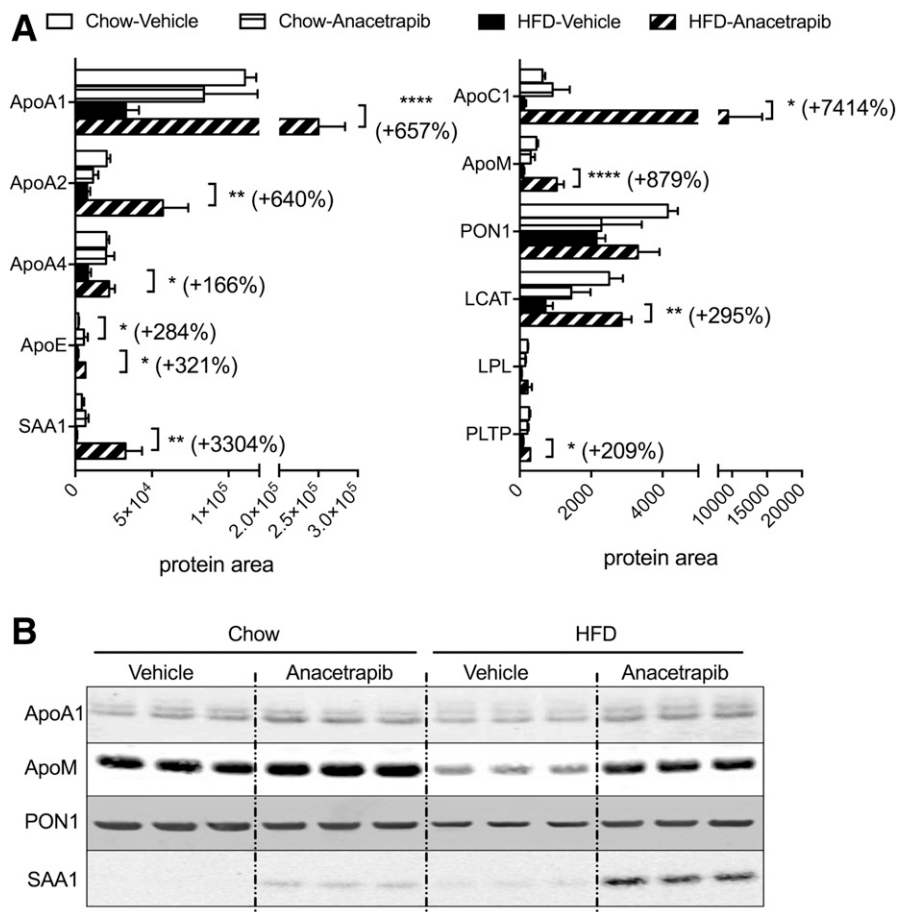


Figure 3—HDL protein composition and lipoproteins. *A*: HPLC fractions (30–40) for HDL were subjected to proteomic analysis. The amount of peptides under area for each protein was normalized by total protein amounts of fractions 30–40. *B*: Immunoblotting was performed with combination of HPLC fraction peaks for HDL cholesterol from each sample. Data are mean \pm SD ($n \geq 6$). Significant differences were determined using repeated-measures by both factors two-way ANOVA with Bonferroni multiple comparison test. * $P < 0.05$, ** $P < 0.01$, **** $P < 0.0001$.

the immunoblot results of protein amounts for apoA1, apoM, PON1, and SAA1 in HDL particles (Fig. 3B).

Enzyme activities of LCAT, lipases, and PLTP also may be regulators for HDL remodeling and function. Blood LCAT enzymatic activity was not affected by diet or anacetrapib (Table 1), whereas LCAT mass in HDL was increased by anacetrapib in HFD-fed mice (Fig. 3A). Blood enzyme activity for total lipases and activity for PLTP were increased by HFD feeding but were not affected by CETP inhibition (Table 1). However, protein levels of LPL and PLTP in HDL particles were slightly lower in HFD-fed mice, and CETP inhibition increased PLTP in HDL particles in HFD-fed mice (Fig. 3A). The results suggest that the distributions of LCAT, lipases, and PLTP between HDL and other lipoprotein particles may be influenced by CETP inhibition, depending on diet.

CETP Inhibition by Anacetrapib Modifies HDL Function

To test the anti-inflammatory effect of HDL, we treated endothelial cells with oxLDL and HDL, and then monitored the expression of endothelial adhesion molecules. Diet did not affect the anti-inflammatory effect of HDL

(Fig. 4A). HDL particles isolated from anacetrapib-treated HFD-fed mice had increased mRNA levels for chemokine (C-C motif) ligand 2 (CCL2) by 92% and intercellular adhesion molecule 1 (ICAM1) mRNA levels by 109% in endothelial cells compared with HDLs from vehicle-treated HFD-fed mice (Fig. 4A). There was no difference for mRNA levels of vascular cell adhesion molecule 1 (VCAM1) between the treatment of HDLs from anacetrapib- and vehicle-treated HFD-fed mice. The capacity for cellular cholesterol efflux was decreased after HFD feeding (Fig. 4B). Anacetrapib did not increase HDL's capacity to accept cellular cholesterol in chow-fed mice (Fig. 4B) but increased cholesterol efflux capacity significantly in HFD-fed mice (Fig. 4B). With regard to the antioxidative function of HDL, HFD feeding decreased HDL antioxidative capacity by shifting the curve toward the left compared with chow (Fig. 4C). Anacetrapib improved the antioxidative function of HDL in HFD-fed mice by shifting the curve close to the one for chow-vehicle mice (Fig. 4C). The area under the curve (AUC) indicates the total formation of conjugated dienes, the oxidation products of LDL, between $t = 0$ and

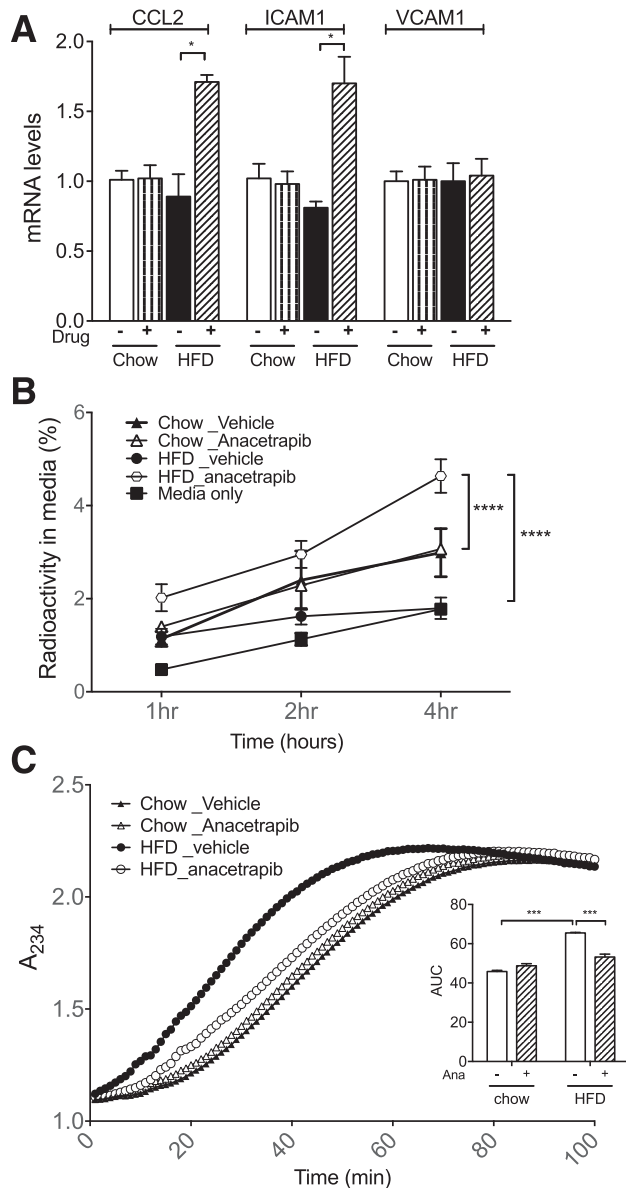


Figure 4—Inhibition of CETP activity by anacetrapib modified HDL function. **A:** Anti-inflammatory effect of HDL particles. **B:** HDL capacity for cellular cholesterol efflux. **C:** Antioxidative function of HDL particles from each group was assessed as the ability to suppress LDL-oxidation. Significant differences were determined using repeated-measures by both factors two-way ANOVA with Bonferroni multiple comparison test ($n \geq 6$ for each group). * $P < 0.05$, *** $P < 0.001$, **** $P < 0.0001$. A_{234} , absorbance reading at 234 nm; Ana, anacetrapib.

90 min when the production leveled off. HFD feeding increased the AUC compared with chow-vehicle mice, and anacetrapib treatment decreased the AUC for LDL oxidants compared with HFD-vehicle mice (Fig. 4C). Thus, anacetrapib treatment increased HDL cholesterol, cholesterol efflux capacity, and antioxidative capacity to a greater degree in HFD-fed mice than in chow-fed mice. However, HFD feeding was associated with insulin resistance and impairment in HDL's anti-inflammatory effects with anacetrapib treatment compared with chow-fed mice.

CETP Inhibition Causes TG Accumulation and Inflammation in the Liver and Exacerbates Insulin Resistance in Diet-Induced Obese Mice

Liver TG content was increased by 475% in diet-induced obese mice compared with chow-fed mice ($P < 0.01$) (Fig. 5A). Anacetrapib further increased liver TGs by 178% compared with vehicle treatment in HFD-fed mice, which was not seen in chow-fed mice ($P < 0.001$) (Fig. 5A). Liver NEFA content was increased by 50% with HFD feeding and further increased by 28% by CETP inhibition in HFD-fed mice ($P < 0.05$) (Fig. 5B). Liver content of diacylglycerol (DG) and cholesterol also was increased by HFD feeding and were not changed by anacetrapib treatment (Fig. 5C and D). Liver content of phospholipids was not different between groups (Fig. 5E). In HFD-fed mice, VLDL-TG secretion was higher in anacetrapib-treated mice at the first 30 min after tyloxapol administration, whereas total TGs over the 3 h were not different between anacetrapib and vehicle-treated mice (Fig. 5F).

To see whether lipid accumulation was associated with inflammation in the liver, we evaluated mRNA levels of inflammation markers. SAA1 mRNA level was increased by 185% by HFD feeding and by 105% and 75% by anacetrapib in chow- and HFD-fed mice, respectively ($P < 0.05$) (Fig. 5G), consistent with changes of serum SAA1 protein levels seen in Fig. 1. Liver IL-6 mRNA level was increased only by CETP inhibition in HFD-fed mice ($P < 0.05$) (Fig. 5H) consistent with the increased IL-6 levels in blood (Table 1). Tumor necrosis factor (TNF)- α mRNA level was increased by 36% by HFD feeding and further increased by 41% by anacetrapib in HFD-fed mice ($P < 0.05$) (Fig. 5I). These data suggest that CETP inhibition with anacetrapib increases liver inflammation in addition to promoting liver TG accumulation in diet-induced obese CETP mice.

CETP Inhibition Modifies Hepatic Lipid Metabolism

To understand the mechanism for liver TG accumulation with anacetrapib in the setting of HFD feeding, we investigated pathways for liver TG metabolism. DG O-acyltransferase 1 (DGAT1) protein amounts were increased with HFD feeding, and anacetrapib did not affect DGAT1 protein expression in either chow- or HFD-fed mice (Fig. 6A and B). DGAT2 protein amounts were increased with HFD feeding and with anacetrapib treatment in both chow- and HFD-fed mice (Fig. 6A and C). Stearoyl-CoA desaturase 1 (SCD1) protein had a similar pattern with anacetrapib treatment as DGAT2 (Fig. 6A and D) likely because they coordinate aspects of TG synthesis and are coordinately regulated at transcriptional and posttranscriptional levels (32). Carnitine palmitoyltransferase 1 (CPT1) transports fatty acids into mitochondria for β -oxidation, a process that is inhibited by malonyl-CoA (32). Liver CPT1 protein amounts were increased by HFD, and anacetrapib treatment limited the increase in HFD-fed mice, which was not seen in chow-fed mice (Fig. 6A and F). The ratio of phosphoryl acetyl-CoA carboxylase

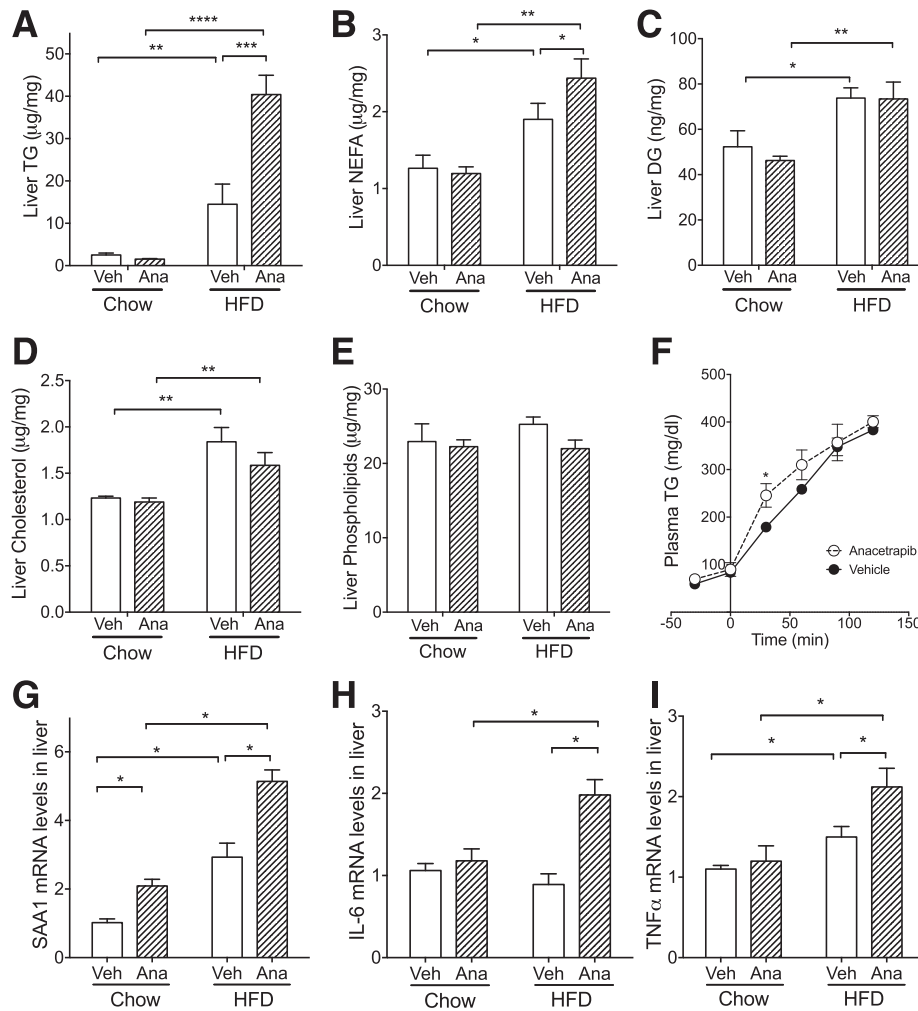


Figure 5—CETP inhibition increased liver lipid content, which was associated with increased inflammation in HFD-fed mice. *A–E*: Liver content for TG, NEFA, DGs, cholesterol, and phospholipids. *F*: VLDL production rates were determined with CETP male mice that were fed an HFD for 1 month and treated with anacetrapib or vehicle. *G–I*: mRNA levels for SAA1, IL-6, and TNF α were determined by real-time PCR. mRNA levels in vehicle-treated chow-fed mice were set as 1. Data are mean \pm SD ($n \geq 6$). Significant differences were determined using two-way ANOVA with Bonferroni multiple comparison test. * $P < 0.05$, ** $P < 0.01$, *** $P < 0.001$, **** $P < 0.0001$. Ana, anacetrapib; Veh, vehicle.

(pACC) to ACC indicates the NEFA flow for β -oxidation because phosphorylation of ACC deactivates its enzymatic activity and leads to the reduction of malonyl-CoA. This ratio was not significantly altered by diet or anacetrapib treatment (Fig. 6*A* and *E*). Microsomal triglyceride transfer (MTP) protein facilitates the addition of a TG droplet onto apoB for VLDL assembly and TG export from liver (26). MTP protein amounts were decreased by HFD and further decreased by anacetrapib treatment in HFD-fed mice, which was consistent with insulin resistance that was represented by fatty liver and increased C-peptide in this group (Figs. 1*C* and 6*A* and *H*). Liver apoB amounts were increased by HFD and were not modified by anacetrapib treatment (Fig. 6*A* and *G*). Hepatocyte fatty acid oxidation was suppressed by HFD and further suppressed by anacetrapib in HFD-fed mice (Fig. 6*I*). These results suggest that anacetrapib

treatment results in fatty liver with HFD feeding by increasing fatty acid delivery to the liver (increased serum fatty acid levels) (Fig. 1*B*) coupled with impairing fatty acid oxidation capacity.

To study whether anacetrapib has similar effects for lipid metabolism in adipose tissue as in the liver, mRNA levels of genes in lipid metabolic pathways were measured. mRNA levels for fatty acid synthase (FASN) were increased by anacetrapib in visceral and brown fat tissues, whereas mRNA levels of DGAT2 were increased by anacetrapib in subcutaneous and visceral fat tissues after hyperinsulinemic clamp (Supplementary Fig. 2). These changes were not seen during fasting in the first cohort mice (data not shown). However, the fatty acid transport protein (FATP) was increased by anacetrapib in brown fat tissues during fasting in diet-induced obese CETP mice (Supplementary Fig. 3*I*).

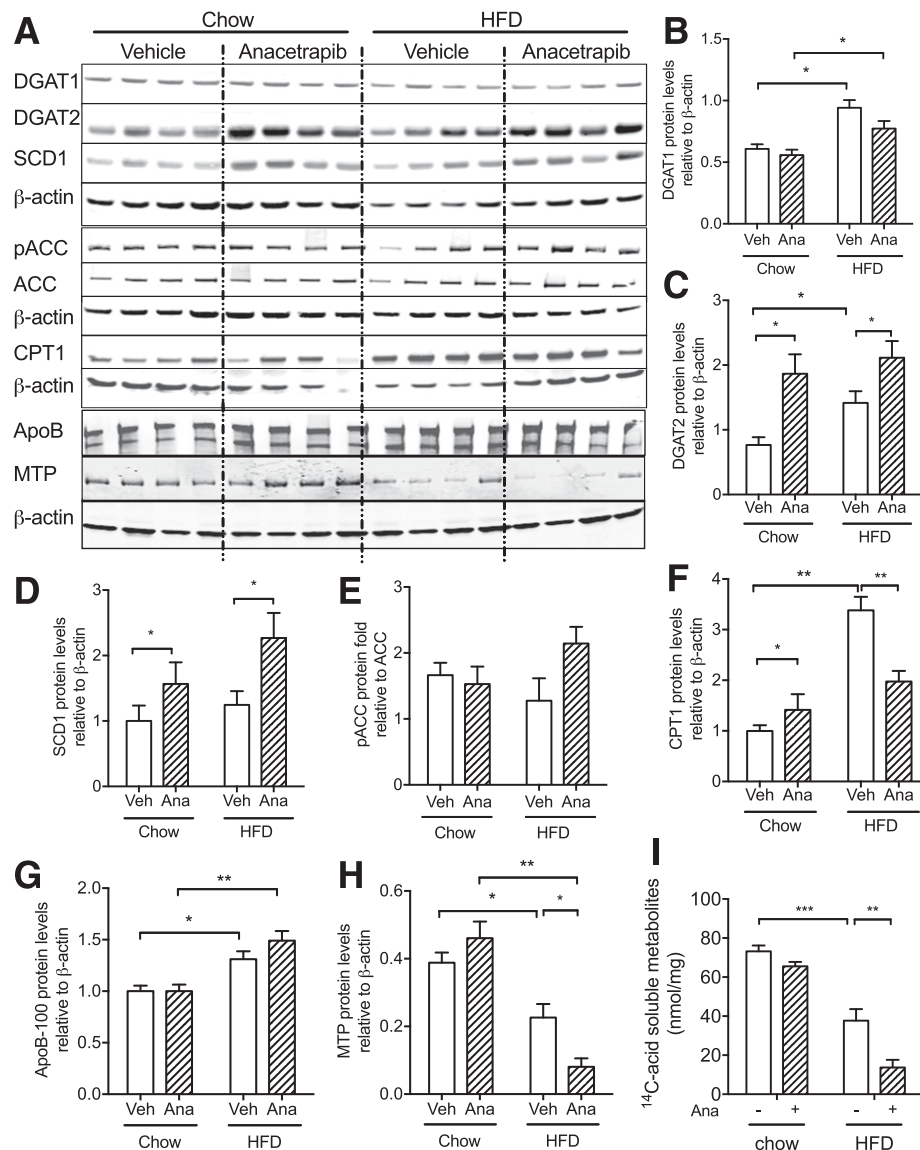


Figure 6—CETP inhibition promoted TG synthesis and impaired fatty acid oxidation in the liver in HFD-fed CETP mice. *A*: Western blots of liver DGAT1, DGAT2, SCD1, pACC, ACC, CPT1, apoB, and MTP from chow- and HFD-fed mice. β -actin was used as the loading control. *B–D*, *F–H*: Quantification of Western blots for each protein. *E*: Ratio of pACC to ACC protein amounts in the liver. *I*: Fatty acid oxidation was measured with primary hepatocytes from CETP male mice that were treated with anacetrapib or vehicle. Data are mean \pm SD ($n \geq 6$; $n = 4$ in *I*). Significant differences were determined using repeated-measures by both factors two-way ANOVA with Bonferroni multiple comparison test. * $P < 0.05$, ** $P < 0.01$, *** $P < 0.001$. Ana, anacetrapib; Veh, vehicle.

CETP Inhibition Worsens Insulin Resistance in Diet-Induced Obese CETP Mice

The high blood levels of C-peptide and NEFA suggested that anacetrapib treatment may have caused insulin resistance in HFD-fed mice. To measure insulin sensitivity, the second cohort of mice were fed an HFD for 3 months and then were treated with anacetrapib and subjected to a euglycemic-hyperinsulinemic clamp study. Anacetrapib or vehicle were administered through a jugular vein catheter for 5 days before the clamp study. The glucose infusion rate (GIR) required to maintain euglycemia under hyperinsulinemic conditions, a measure of insulin sensitivity, was significantly lower during the clamp in anacetrapib-treated mice (Fig. 7A

and B). With a similar R_d , the increased hepatic glucose production (endogenous rate of appearance 5.1 vs. 10.4 mg/kg/min; $P < 0.05$) (Fig. 7C and D) during hyperinsulinemia suggested that hepatic insulin resistance was the driver for the whole-body insulin resistance (lower GIR) in anacetrapib-treated obese mice. Hepatic insulin signaling also was blunted by 54% as represented by decreased AKT phosphorylation at ⁴⁷³Ser in those mice ($P < 0.05$) (Fig. 7E and F). Liver TG content and NEFA levels were higher in anacetrapib- than in vehicle-treated mice in the second cohort, wherein other lipid contents in the liver were not changed (Fig. 7G–K). Of note, anacetrapib treatment did not worsen insulin resistance in WT diet-induced obese mice (Supplementary Fig. 6A–E),

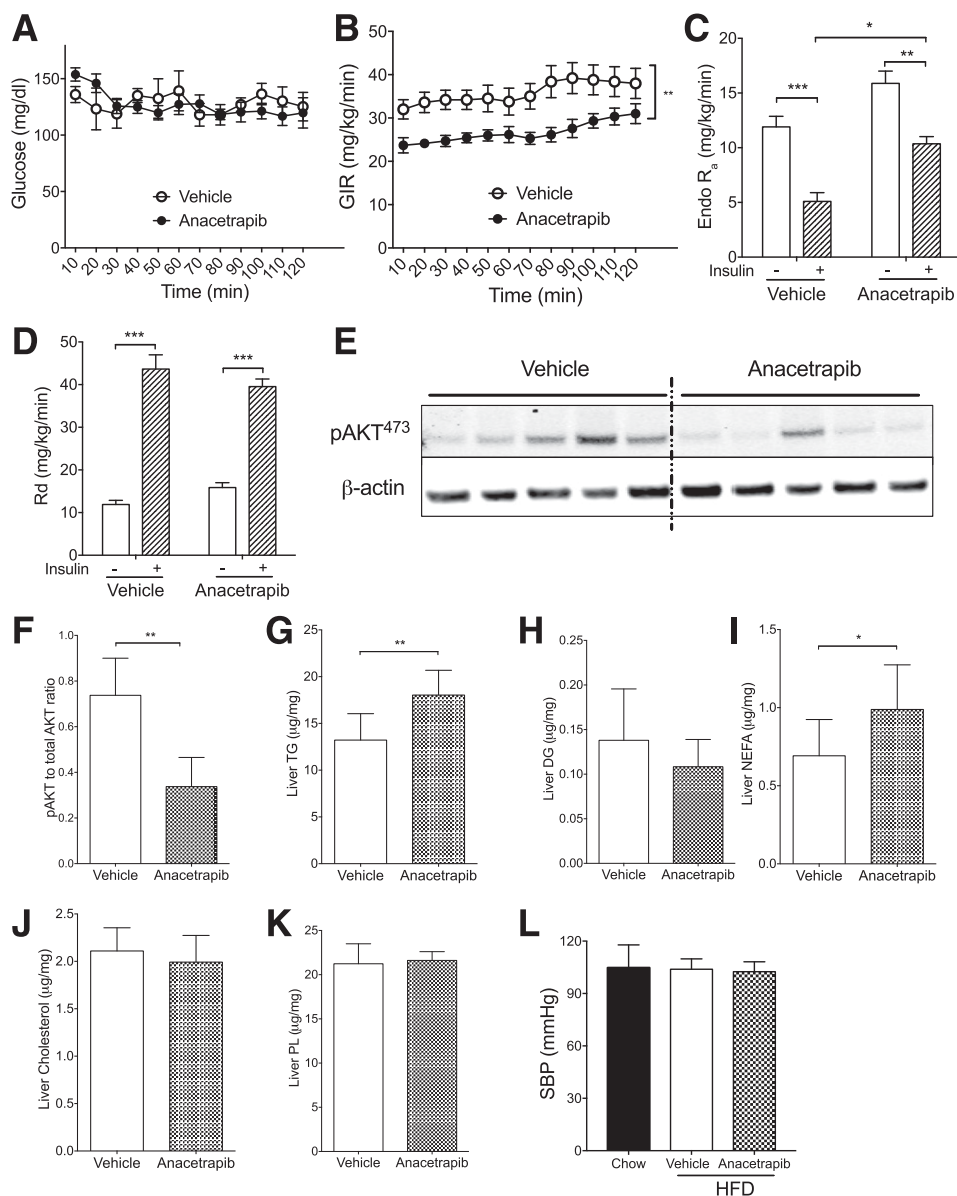


Figure 7—CETP inhibition with anacetrapib worsened insulin resistance in HFD-fed CETP mice. **A**: Euglycemia was maintained at ~150 mg/dL during the clamp. **B**: GIR to maintain euglycemia was lower in anacetrapib-treated mice. **C**: Hepatic glucose production (Endo R_a) was less suppressed by insulin in anacetrapib-treated mice than in vehicle-treated mice. **D**: R_d was increased similarly for both groups by insulin during clamp. **E** and **F**: Insulin-mediated phosphorylation of liver AKT (⁴⁷³Ser) (pAKT⁴⁷³) was decreased in anacetrapib-treated mice shown by immunoblotting and its quantification. **G–K**: Liver content for TG, DG, NEFA, cholesterol, and phospholipids (PL). **L**: SBP for the third cohort of mice. CETP transgenic mice fed a chow diet were used as controls. Data are mean ± SD ($n \geq 6$). Significant differences for **A–D** were determined using two-way ANOVA with Bonferroni multiple comparison test; statistical analyses for **E–L** were by Student *t* test. * $P < 0.05$, ** $P < 0.01$, *** $P < 0.001$.

demonstrating that the effects of anacetrapib to generate insulin resistance require CETP expression. We had previously noted that CETP female mice are protected from insulin resistance with 4 weeks of HFD feeding compared with WT littermates, an effect not seen in males (19). These CETP male mice were not more insulin sensitive than their WT littermates with 3 months of HFD feeding (Supplementary Fig. 6F and G), consistent with our prior results.

Hypertension has been observed in clinical trials with CETP inhibitors (10,33–36). We tested the blood pressure

in a cohort of mice after a longer period of HFD feeding (5 months) and CETP inhibition (3 weeks), then blood pressure was determined as describe previously (37). SBP was not changed by either HFD or CETP inhibition in CETP transgenic mice (Fig. 7L).

DISCUSSION

In this study, we show that CETP inhibition with anacetrapib affects HDL function, the HDL proteome, and metabolic outcomes differently depending on whether

the mice were fed an obesogenic diet versus a chow diet. Anacetrapib treatment of CETP mice increased HDL cholesterol in chow- and HFD-fed mice. Increases in HDL cholesterol did not necessarily improve HDL function in chow-fed mice, which fits a growing consensus that HDL functionality is more predictive than HDL cholesterol levels with regard to protection from CVD. Proteomics technology has provided insight into the connections between HDL protein composition and functionality. We show a marked dietary influence on the modification of the HDL proteome by CETP inhibition with anacetrapib, which contributes to the functionality of HDL. Furthermore, inhibition of CETP in HFD-fed mice increased NEFA in the circulation and the liver and modified control of regulatory steps of TG metabolism in the liver, which was associated with increases in inflammatory markers and whole-body insulin resistance.

CETP inhibition interfered with TG metabolic pathways, leading to liver TG accumulation and insulin resistance in diet-induced obese mice. Together with previous reports that transgenic expression of CETP reduces liver TG content through several novel functions, including promoting lipid oxidation and VLDL-TG production in chow-fed female mice (20) and improved insulin sensitivity in HFD-fed mice (19), we demonstrate an important physiologic role of CETP. CETP facilitates the exchange of cholesterol and TG, but our studies fit into a growing picture showing that CETP has important physiologic functions beyond regulation of HDL cholesterol levels. In hypertriglyceridemic mice of apoA1 background, the addition of CETP suppressed apoA1 synthesis in intestine (38). CETP expression decreased plasma TG in hyperlipidemic LDLR^{-/-} mice (39,40). In this study, effects of CETP inhibition on fatty acid and TG metabolism were more pronounced in obese mice. HDL is the main carrier of apoC1, and apoC1 is a regulator of CETP activity in humans (41). CETP inhibition more strikingly increased apoC1 in HFD-fed than in chow-fed mice, likely leading to serum NEFA elevation, because overexpression of apoC1 increases plasma NEFA (42–44). In addition to increasing TG synthesis through the upregulation of DGAT2 and SCD1, anacetrapib reduced fatty acid oxidation in the liver, likely by suppressing CPT1 levels. The increased fatty liver correlated with increased markers of liver inflammation and liver insulin resistance in our clamp study.

We show that CETP inhibition with anacetrapib increases systemic and hepatic inflammation to a greater degree in obese mice than in chow-fed mice. We note that CETP activity from blood of CETP mice was about twice as high as that from human blood (Supplementary Fig. 7B). We do not know whether this relative overexpression of CETP affects our findings, but note that CETP inhibitors have raised plasma levels of high-sensitivity C-reactive protein, a biomarker of systemic inflammation, in clinical trials with torcetrapib, dalcetrapib, and evacetrapib (33–35). In mice, CETP inhibition by torcetrapib reduces

atherosclerotic lesion size but increases proinflammatory responses in lesions that predisposed the lesion for thrombosis (45). In this study, CETP inhibition increased SAA1 in the liver and increased IL-6 when the burden for lipid metabolism was higher in HFD-fed obese mice. The contribution of SAA1 and IL-6 from the liver to the blood further impaired HDL function to protect endothelial cells from oxLDL-induced inflammation.

Most recently, a clinical trial with a longer follow-up showed that anacetrapib reduces CVD risk, an effect that was likely attributable mostly to decreases in LDL cholesterol (10,36). Using mouse models with minimal interruption from changes other than HDL, we show that HDL particles generated by CETP inhibition promote beneficial functionalities, such as cholesterol efflux and antioxidative action, specifically in diet-induced obese mice. However, CETP inhibition promoted hepatic TG accumulation and caused insulin resistance in the same group of mice, which may counterbalance the benefits on clinical outcomes induced by CETP inhibitors. The findings from the current study are helpful with regard to understanding the physiologic importance of CETP expression and the complex effects of CETP inhibitors in clinical trials. In addition, in an era of personalized medicine, this study suggests that consideration of obesity and diet as potential modifiers of the effects of drugs used to prevent and treat CVD might be valuable.

Funding. This study was supported by the Vanderbilt Hormone Assay Core (NIH grant DK-020593), Vanderbilt Mouse Metabolic Phenotyping Core (NIH grant DK-59637), Vanderbilt Diabetes Research and Training Center (P30-DK-020593 and P30-DK-058404), and Vanderbilt O'Brien Kidney Center (DK-114809). S.F. was supported by NIH grant R01-HL-132985, and J.M.S. was supported by the Department of Veterans Affairs (BX002223) and NIH grant R01-DK-109102.

Duality of Interest. No potential conflicts of interest relevant to this article were reported.

Author Contributions. L.Z. wrote the manuscript and researched data. T.L., C.H.E., B.A.P., J.S., E.T., F.Z., and Z.K. researched data and reviewed the manuscript. R.C.H. and D.H.W. reviewed and edited the manuscript. S.F. contributed to the discussion and reviewed and edited the manuscript. J.M.S. researched data, contributed to the discussion, and reviewed and edited the manuscript. J.M.S. is the guarantor of this work and, as such, had full access to all the data in the study and takes responsibility for the integrity of the data and the accuracy of the data analysis.

References

1. Kingwell BA, Chapman MJ, Kontush A, Miller NE. HDL-targeted therapies: progress, failures and future. *Nat Rev Drug Discov* 2014;13:445–464
2. Qin X, Swertfeger DK, Zheng S, Hui DY, Tso P. Apolipoprotein AIV: a potent endogenous inhibitor of lipid oxidation. *Am J Physiol* 1998;274:H1836–H1840
3. Peng N, Meng N, Wang S, et al. An activator of mTOR inhibits oxLDL-induced autophagy and apoptosis in vascular endothelial cells and restricts atherosclerosis in apolipoprotein E^{-/-} mice. *Sci Rep* 2014;4:5519
4. Kita T, Kume N, Minami M, et al. Role of oxidized LDL in atherosclerosis. *Ann N Y Acad Sci* 2001;947:199–205; discussion 205–206
5. Tran-Dinh A, Diallo D, Delbosc S, et al. HDL and endothelial protection. *Br J Pharmacol* 2013;169:493–511

6. Lamarche B, Uffelman KD, Carpentier A, et al. Triglyceride enrichment of HDL enhances in vivo metabolic clearance of HDL apo A-I in healthy men. *J Clin Invest* 1999;103:1191–1199
7. Barter PJ, Caulfield M, Eriksson M, et al.; ILLUMINATE Investigators. Effects of torcetrapib in patients at high risk for coronary events. *N Engl J Med* 2007;357:2109–2122
8. Kastelein JJ, van Leuven SI, Burgess L, et al.; RADIANCE 1 Investigators. Effect of torcetrapib on carotid atherosclerosis in familial hypercholesterolemia. *N Engl J Med* 2007;356:1620–1630
9. Lincoff AM, Nicholls SJ, Riesmeyer JS, et al.; ACCELERATE Investigators. Evacetrapib and cardiovascular outcomes in high-risk vascular disease. *N Engl J Med* 2017;376:1933–1942
10. Bowman L, Hopewell JC, Chen F, et al.; HPS3/TIMI55–REVEAL Collaborative Group. Effects of anacetrapib in patients with atherosclerotic vascular disease. *N Engl J Med* 2017;377:1217–1227
11. Fazio S, Linton MF. Killing two birds with one stone, maybe: CETP inhibition increases both high-density lipoprotein levels and insulin secretion. *Circ Res* 2013;113:94–96
12. Khera AV, Wolfe ML, Cannon CP, Qin J, Rader DJ. On-statin cholesteryl ester transfer protein mass and risk of recurrent coronary events (from the pravastatin or atorvastatin evaluation and infection therapy–thrombolysis in myocardial infarction 22 [PROVE IT–TIMI 22] study). *Am J Cardiol* 2010;106:451–456
13. Ritsch A, Scharnagl H, Eller P, et al. Cholesteryl ester transfer protein and mortality in patients undergoing coronary angiography: the Ludwigshafen Risk and Cardiovascular Health study. *Circulation* 2010;121:366–374
14. Robins SJ, Lyass A, Brocia RW, Massaro JM, Vasan RS. Plasma lipid transfer proteins and cardiovascular disease. The Framingham Heart Study. *Atherosclerosis* 2013;228:230–236
15. Forrester JS, Makkar R, Shah PK. Increasing high-density lipoprotein cholesterol in dyslipidemia by cholesteryl ester transfer protein inhibition: an update for clinicians. *Circulation* 2005;111:1847–1854
16. Marotti KR, Castle CK, Boyle TP, Lin AH, Murray RW, Melchior GW. Severe atherosclerosis in transgenic mice expressing simian cholesteryl ester transfer protein. *Nature* 1993;364:73–75
17. Hayek T, Masucci-Magoulas L, Jiang X, et al. Decreased early atherosclerotic lesions in hypertriglyceridemic mice expressing cholesteryl ester transfer protein transgene. *J Clin Invest* 1995;96:2071–2074
18. Bérard AM, Föger B, Remaley A, et al. High plasma HDL concentrations associated with enhanced atherosclerosis in transgenic mice overexpressing lecithin-cholesteryl acyltransferase. *Nat Med* 1997;3:744–749
19. Cappel DA, Palmisano BT, Emfinger CH, Martinez MN, McGuinness OP, Stafford JM. Cholesteryl ester transfer protein protects against insulin resistance in obese female mice. *Mol Metab* 2013;2:457–467
20. Palmisano BT, Le TD, Zhu L, Lee YK, Stafford JM. Cholesteryl ester transfer protein alters liver and plasma triglyceride metabolism through two liver networks in female mice. *J Lipid Res* 2016;57:1541–1551
21. Tan EY, Hartmann G, Chen Q, et al. Pharmacokinetics, metabolism, and excretion of anacetrapib, a novel inhibitor of the cholesteryl ester transfer protein, in rats and rhesus monkeys. *Drug Metab Dispos* 2010;38:459–473
22. Zhu L, Shi J, Luu TN, et al. Hepatocyte estrogen receptor alpha mediates estrogen action to promote reverse cholesterol transport during Western-type diet feeding. *Mol Metab* 2018;8:106–116
23. Toth CA, Kuklenyik Z, Jones JI, et al. On-column trypsin digestion coupled with LC-MS/MS for quantification of apolipoproteins. *J Proteomics* 2017;150:258–267
24. Zhu L, Giunzioni I, Tavori H, et al. Loss of macrophage low-density lipoprotein receptor-related protein 1 confers resistance to the antiatherogenic effects of tumor necrosis factor- α inhibition. *Arterioscler Thromb Vasc Biol* 2016;36:1483–1495
25. Zhu L, Brown WC, Cai Q, et al. Estrogen treatment after ovariectomy protects against fatty liver and may improve pathway-selective insulin resistance. *Diabetes* 2013;62:424–434
26. Swift LL, Zhu MY, Kakkad B, et al. Subcellular localization of microsomal triglyceride transfer protein. *J Lipid Res* 2003;44:1841–1849
27. Hirschey MD, Verdin E. Measuring fatty acid oxidation in tissue homogenates. *Protoc Exch* 2010;2010:631
28. Brodeur MR, Rhoads D, Charpentier D, et al. Dalcetrapib and anacetrapib differently impact HDL structure and function in rabbits and monkeys. *J Lipid Res* 2017;58:1282–1291
29. Barter PJ, Rye KA, Tardif JC, et al. Effect of torcetrapib on glucose, insulin, and hemoglobin A1c in subjects in the Investigation of Lipid Level Management to Understand its Impact in Atherosclerotic Events (ILLUMINATE) trial. *Circulation* 2011;124:555–562
30. Siebel AL, Natoli AK, Yap FY, et al. Effects of high-density lipoprotein elevation with cholesteryl ester transfer protein inhibition on insulin secretion. *Circ Res* 2013;113:167–175
31. Barter P, Gotto AM, LaRosa JC, et al.; Treating to New Targets Investigators. HDL cholesterol, very low levels of LDL cholesterol, and cardiovascular events. *N Engl J Med* 2007;357:1301–1310
32. Postic C, Girard J. Contribution of de novo fatty acid synthesis to hepatic steatosis and insulin resistance: lessons from genetically engineered mice. *J Clin Invest* 2008;118:829–838
33. Cannon CP, Shah S, Dansky HM, et al.; Determining the Efficacy and Tolerability Investigators. Safety of anacetrapib in patients with or at high risk for coronary heart disease. *N Engl J Med* 2010;363:2406–2415
34. Nicholls SJ, Brewer HB, Kastelein JJ, et al. Effects of the CETP inhibitor evacetrapib administered as monotherapy or in combination with statins on HDL and LDL cholesterol: a randomized controlled trial. *JAMA* 2011;306:2099–2109
35. Schwartz GG, Olsson AG, Abt M, et al.; dal-OUTCOMES Investigators. Effects of dalcetrapib in patients with a recent acute coronary syndrome. *N Engl J Med* 2012;367:2089–2099
36. Holmes MV, Smith GD. Dyslipidaemia: revealing the effect of CETP inhibition in cardiovascular disease. *Nat Rev Cardiol* 2017;14:635–636
37. Zeng F, Kloepper LA, Finney C, Diedrich A, Harris RC. Specific endothelial heparin-binding EGF-like growth factor deletion ameliorates renal injury induced by chronic angiotensin II infusion. *Am J Physiol Renal Physiol* 2016;311:F695–F707
38. Hayek T, Azrolan N, Verdery RB, et al. Hypertriglyceridemia and cholesteryl ester transfer protein interact to dramatically alter high density lipoprotein levels, particle sizes, and metabolism. Studies in transgenic mice. *J Clin Invest* 1993;92:1143–1152
39. Casquero AC, Berti JA, Salerno AG, et al. Atherosclerosis is enhanced by testosterone deficiency and attenuated by CETP expression in transgenic mice. *J Lipid Res* 2006;47:1526–1534
40. Cazita PM, Berti JA, Aoki C, et al. Cholesteryl ester transfer protein expression attenuates atherosclerosis in ovariectomized mice. *J Lipid Res* 2003;44:33–40
41. de Barros JP, Boualam A, Gautier T, et al. Apolipoprotein C1 is a physiological regulator of cholesteryl ester transfer protein activity in human plasma but not in rabbit plasma. *J Lipid Res* 2009;50:1842–1851
42. Jong MC, Gijbels MJ, Dahlmans VE, et al. Hyperlipidemia and cutaneous abnormalities in transgenic mice overexpressing human apolipoprotein C1. *J Clin Invest* 1998;101:145–152
43. Jong MC, Voshol PJ, Muurling M, et al. Protection from obesity and insulin resistance in mice overexpressing human apolipoprotein C1. *Diabetes* 2001;50:2779–2785
44. Muurling M, van den Hoek AM, Mensink RP, et al. Overexpression of APOC1 in obob mice leads to hepatic steatosis and severe hepatic insulin resistance. *J Lipid Res* 2004;45:9–16
45. de Haan W, de Vries-van der Weij J, van der Hoorn JW, et al. Torcetrapib does not reduce atherosclerosis beyond atorvastatin and induces more proinflammatory lesions than atorvastatin. *Circulation* 2008;117:2515–2522